MEASURING SURFACE URBAN HEAT ISLAND IN RESPONSE TO POPULATION DENSITY BASED ON REMOTE SENSING DATA AND GIS TECHNIQUES: APPLICATION TO PRISHTINA, KOSOVO

Albert BERILA [A], **Mimoza DUSHI** [B*]

Received: July 28, 2021 | Revised: October 25, 2021 | Accepted: October 27, 2021
Paper No. 21-63/2-608

Abstract

Urban areas, compared to rural areas, have much more visible characteristics of their climate, such as higher surface and air temperatures, and large spatial variation – within the city – of meteorological parameters. The study aimed at investigating the phenomenon of the Surface Urban Heat Island (SUHI) over the Municipality of Prishtina, Kosovo. The SUHI was investigated based on the relationship between Land Surface Temperature (LST) estimated from Landsat 8 Thermal Infrared Sensor (TIRS) band with population density using Geographic Information System (GIS). To understand the relationship between population density and Land Surface Temperature (LST), we performed a correlation analysis. This analysis showed a strong positive relationship with a value of r = 0.768005, emphasizing the strong role that the population has in creating areas that generate the SUHI effect. Also, the results of the study clearly showed that built-up areas and bare surfaces are responsible for generating the SUHI effect, while vegetation and water bodies minimize this effect by creating freshness. The study showed that Land Surface Temperature increases with the increase of impervious surfaces, which is related to the increase of population density. Maps in which the identification of the SUHI effect is presented can be a very useful tool for urban administration as well as for urban planning policies for the latter to be directed exactly in those areas where this phenomenon is present and causes a range of concerns for citizens.

Key words

GIS, Remote Sensing, SUHI, LST, population density, Municipality of Prishtina.

INTRODUCTION

In many scientific studies around the world, in recent times and decades, one thing that stands out with great importance – at the center of many studies – is climate variability and climate change. We are witnessing that, currently, from various an-

A University of Prishtina, 10000, Prishtina, Republic of Kosovo
https://orcid.org/0000-0003-0754-269X
albert.berila@outlook.com

B* University of Prishtina, 10000, Prishtina, Republic of Kosovo
https://orcid.org/0000-0002-1853-6829
mimoza.dushi@uni-pr.edu (corresponding author)

thropogenic/natural activities, our planet is experiencing significant environmental changes. Human – since its first appearance – has tried to use/adapt all the riches of our planet constantly depending on the emergence of his needs. We are very aware that the human is part of the planet Earth/nature, but it should also be noted that, unlike other living things, human has made and continues to make radical changes around, thus creating the cultural environment (Isufi and Berila, 2021).

Recently, global urbanization – in much of the world – is undergoing extraordinary expansion as a result of massive population growth (Berila and Isufi, 2021b). A fair/correct development of urbanization means positive urbanization, but when this does not happen, negative effects appear on human health and in our environment (Morefield et al. 2018; Berila and Isufi, 2021b). All this massive increase in urbanization can not pass without any negative effect. Some of the negative effects include increased density of built-up areas; replacement of natural surfaces with artificial surfaces (an increase of impervious surfaces); lack of green spaces etc. The causes that have influenced the cities to have higher temperatures than their suburban areas are human and industrial activities that take place in urban areas, then buildings, concrete, and asphalt. All these changes have influenced the appearance of a phenomenon called UHI. The term UHI was first used in 1818. The notion of UHI represents the phenomenon in which the urban surface and atmospheric temperature are higher compared to the surrounding environment – suburban areas (non-urban) (Wang et al. 2017). Nowadays more than 50% of the world's population lives in urban areas and with the current trend, the number of people who will live in urban areas will increase day by day. Thus, it is expected that by 2030 more than 60% of people will live in these areas and, 1 in 3 people will live in cities that will have at least half a million inhabitants (UN, 2016). Therefore, it should be rightly said that the UHI phenomenon is a global concern, which will threaten the functioning and population of our cities (Mohajerani et al. 2017) and, not only that, negative actions and implications will also appear in urban planning; air pollution; human health and comfort; but also in energy management (Peres et al. 2018).

The UHI effect occurs when the land cover is transformed, mainly when replacing agricultural lands and natural vegetation with surfaces that are impervious, such as asphalt, concrete, roofs, walls of buildings (Buyantuyev and Wu, 2009), etc. The effects of UHI are quite negative and include increased energy consumption, increased emissions of air pollutants, increased emissions of greenhouse gases, damage to water quality, and the creation of harmful environmental conditions that negatively affect health and human comfort (EPA, 2017).

Urbanization processes and improper and unplanned urban planning is the cause of the UHI effect (Nuruzzaman, 2017). Such processes create dense buildings and surfaces with asphalt and concrete, which have heat-retaining capabilities (Harlan and Ruddell, 2011; Mavrogianni et al. 2011). In the end, the result of all this is the increase in high heat emissions (Santamouris et al. 2011) and increasing the demand and need for energy in order to cool the buildings. In addition, a direct active role in enhancing the UHI effect is played by the increase in density and height of buildings on both sides of the road creating what is known as urban road canyons; reduction of areas planted with vegetation (lack of green areas); increasing use of low albedo materials (high heat absorption) (Taha, 1997); reduction of wind speed due to the geometric shape created as a result of the construction of buildings in the city (O'Malley et al. 2014), etc. The study of this phenomenon is extremely important. Understanding the origin and consequences of this phenomenon and finding ways to prevent the expansion and intensity of it should be a priority for city managers and urban planners.

Urban Heat Island phenomena can be studied in three urban layers (Fabrizi et al. 2010; Sherafati et al. 2018):

1) Canopy Layer Heat Island (CLHI) – this layer lies approximately at the average height of buildings and is determined by measuring the air temperature at a height of 2 m above the ground. The CLHI has usually measured through sensors mounted on fixed meteorological stations (Nichol et al. 2006; Schwarz et al. 2012; Smoliak et al. 2015; Clay et al. 2016).
2) Boundary Layer Heat Island (BLHI) – lies above the CLHI layer and can reach a thickness of up to 1 km. It is measured using special platforms, such as radiosondes and aircraft (Voogt, 2008; Sherafati et al. 2018).
3) Surface Urban Heat Island (SUHI) – difference in radiant temperature between urban and non-urban surfaces. The measurement/determination of this layer is done using thermal remote sensors (Voogt and Oke, 2003).

Accurate measurement of the UHI effect can be done through meteorological stations. However, accurate data obtained from thermometers placed at ground stations cannot be used due to spatial constraints. More precisely, the reason for the small/insufficient number of the spatial distribution of meteorological stations and their inhomogeneity has made the data obtained insufficient to study the UHI effect. The SUHI and UHI phenomena are closely related to each other and, simply put, the SUHI represents an indirect assessment of UHI (Schwarz et al. 2012). In the scientific literature, there are a series of scientific papers which show that to study the SUHI phenomenon they have used LST, while to study the UHI phenomenon, usually, air temperature data have been used (Voogt and Oke, 2003; Despini et al. 2016; Pour and Voženílek, 2020). The development of Remote Sensing has made it possible for the SUHI phenomenon to be studied through the calculation of LST and, that is why in our study we have chosen to analyze the SUHI phenomenon. Due to functions such as data management, calculating, analyzing and creating an important database, geospatial technology offers great support in such research

(Berila and Isufi, 2021a) as the measurement of the SUHI phenomenon.The difference between CLHI and BLHI compared to SUHI is that atmospheric UHIs (CLHI and BLHI) are higher at night (have higher values), while surface UHIs (SUHI) are higher (larger) during the day (Roth et al. 1989; Yuan and Bauer, 2007). All dry urban surfaces and those that have a low albedo value (absorb heat) have the ability to heat more (have a higher temperature) than the air temperature. Therefore, based on this, the values of SUHI will not only be higher during the day but, consequently, the intensity of SUHI will be greater during the summer season compared to other seasons. It is precisely the dry weather conditions and the changes in solar radiation that cause such a thing to come/appear (Oke, 1987). Given all the above effects that the SUHI phenomenon can cause, for people to live in areas that are healthy, suitable for living, and sustainable in urban terms, good governance and urban planning are necessary. Such a thing cannot be done if the city administrators do not have an idea of how to identify SUHI. Given that the areas where the phenomenon SUHI appears create great concerns for residents, it is more than necessary to direct all urban policies in these areas in order to reduce such a phenomenon as much as possible.

The increase in carbon emissions and the appearance of climate change is due to the increase in the number of urban inhabitants – variability in consumption and production patterns (UNHABITAT, 2016). The most affected by a series of negative events, such as pressure/housing needs, increased pollution, and traffic jams are developing countries (Lee and Chang, 2011; Mubea et al. 2011; Kityuttachai et al. 2013; Berila and Isufi, 2021b). Another very important thing to note which is the cause of urbanization and strengthening of urban morphology is the loss of biodiversity – irreversible loss (Sudhira et al. 2003; Kamusoko and Aniya, 2007; Kamusoko et al. 2009; Liu et al. 2011; Moghadam and Helbich, 2013; Berila and Isufi, 2021b). Normally, such a process of urbanization, without distinction, includes the cities of the Republic of Kosovo – with special emphasis on Prishtina. Urban growth has occurred in it as a result of natural population growth, migration, and economic development (Berila and Isufi, 2021b).

In our paper the main purpose is to see whether the SUHI phenomenon is empowered in the cadastral zones that have the highest population density; to be able to identify all areas affected by this phenomenon by creating a connection between the atmosphere and LST. Our other goal is to help the Municipality of Prishtina by identifying all areas facing and endangered by the SUHI phenomenon, in order to take action against this phenomenon as soon as possible – for the population to live as healthy as possible.

STUDY AREA

Prishtina is the capital and largest city of the Republic of Kosovo, which lies in the north-eastern part of the country, while within the Balkan Peninsula, it occupies a central position – very convenient (Fig. 1).

About 523 km^2 is the surface of the Municipality of Prishtina. It lies in the morphological plan of Kosovo and represents an alluvial plan covered with sediments of lakes, and geologically it is a tectonic depression, which has risen long Oligo-Miocene changes (Municipality of Prishtina, 2013; Isufi and Berila, 2021). Cold winters, hot summers, with a 600 mm average of rainfall per year, make the climate continental (Municipality of Prishtina, 2013; Isufi and Berila, 2021). The average annual air temperature is 9.9ºC. The highest monthly average air temperature in Prishtina appears in July at 19.8ºC, while the lowest average air temperature appears in January at -1.4ºC (Pllana, 2015). The average annual rainfall is around 600 mm, with the highest monthly average in May and November (68 mm), while the lowest monthly average reaches in February (36 mm) (Pllana, 2015).

In this area, the hilly-mountainous relief occupies the eastern, northeastern, and southeastern parts. The western part has an altitude of 535-580 meters. In general, the slope of the terrain is low – excluding the eastern part (Municipality of

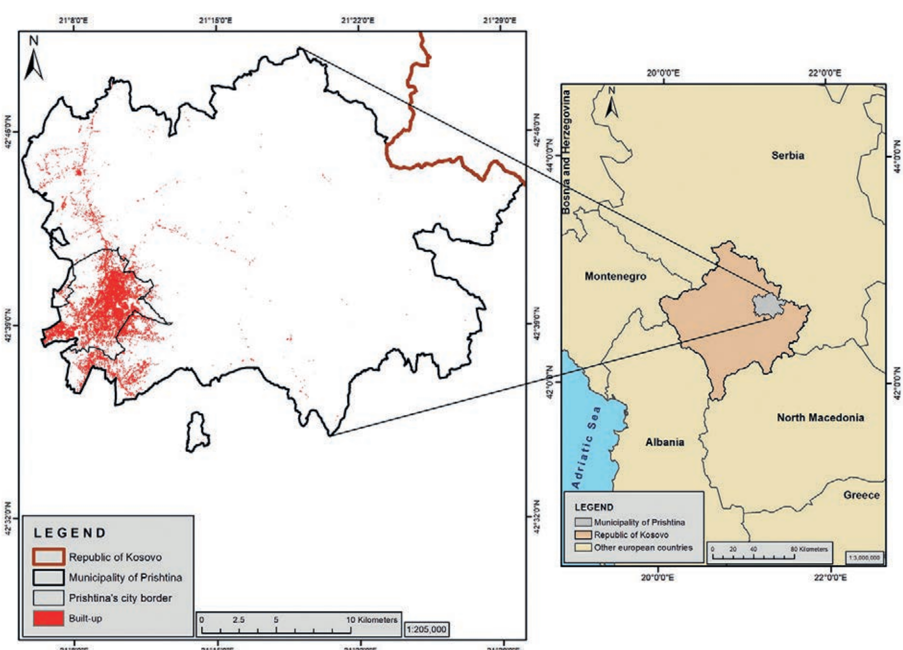

Fig. 1
Location of the study area
Source: Compiled by authors

Prishtina, 2013; Berila and Isufi, 2021b). In addition, this area is also known as the largest administrative, economic and cultural center in Kosovo (Fig. 2). This area has a total of 216,870 inhabitants – referring to the official statistics of 2019 (KAS, 2020). It is worth noting that this area has undergone a major change (transformation), both socially and physically. Unplanned constructions in many areas of the city, the expansion of settlements around the city, and the expansion of the urban area are the reason for such changes to be more visible. After the last war in Kosovo ('99), 11% of Kosovo's population has migrated within the country. The main segment is concentrated around Prishtina, which has gained 23% of all in-migrants (KAS, 2012). As a result of such developments, there was a need for housing, there was a high increase in population density, increased demand for apartments, etc. Finally, the lack of implementation of the municipal development plan due to corruption and political interference also served this uncontrollable development (Berila and Isufi, 2021b).

In many parts of the world, the migration of population from rural to urban areas has created rapid changes towards urban development. In the Republic of Kosovo, such changes, with a special emphasis, have occurred in the last 20 years. The population has migrated from rural to urban areas, and from peripheral are-

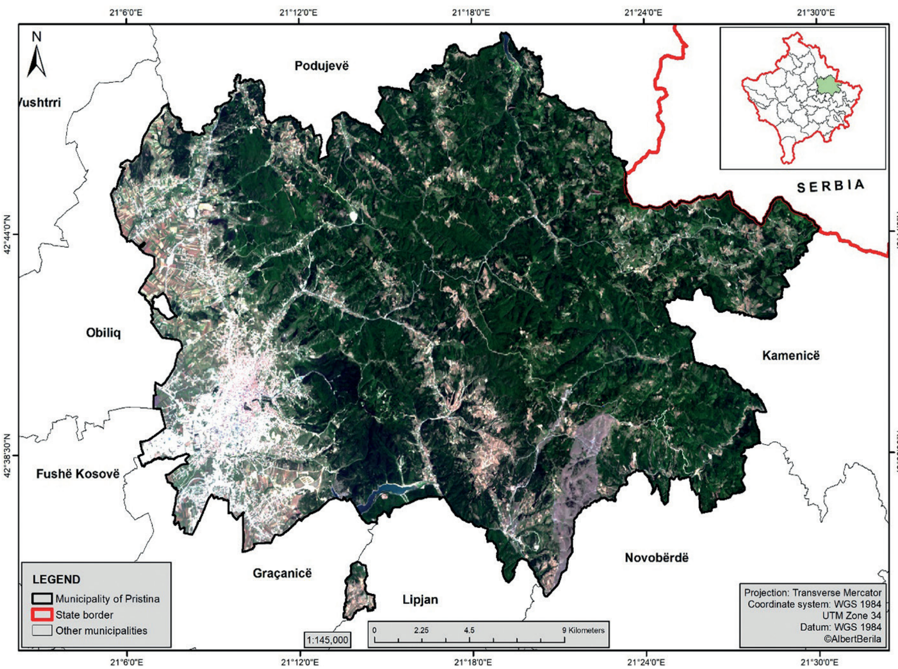

Fig. 2
Satellite image of Prishtina – Landsat 8
Source: Compiled by authors

as to those large cities – especially in Prishtina (KAS, 2014; Isufi and Berila, 2021). The reasons why people decided to leave heading to the capital of Kosovo had to do with finding a better job, getting a better education, and, ultimately, creating a better life. Unfortunately, Kosovo's institutions have been totally unprepared for all these socio-economic developments (Isufi and Berila, 2021).

To this day, it is worth noting that the capital continues to face quite large challenges, which have caused it a lot of trouble. It is about unbalanced development, loss of agricultural land, major problems in infrastructure, and other social problems (Isufi and Berila, 2021).

DATA AND METHODS

Cloud-free Landsat 8 Operational Land Imager/Thermal Infrared Sensors (OLI/TIRS) satellite image for 2nd July 2019 of Path 185 and Row 30 with 0% cloud cover was acquired from the United States Geological Survey (USGS) and used to calculate the Land Surface Temperature (LST). The Landsat 8 satellite was successfully launched on 11 February 2013 and deployed into orbit with two instruments onboard (Valizadeh Kamran et al. 2015): the Operational Land Imager (OLI) and the Thermal Infrared Sensor (TIRS), which jointly produce a multispectral image consisting of 11 spectral bands. OLI collects nine spectral bands including a pan band: bands 1-4 correspond to the visible part of the electromagnetic spectrum, bands 5-7 and 9 to near-infrared and shortwave infrared regions of the spectrum (Taloor et al. 2021) (all of these have a spatial resolution of 30 m) (Jeevalakshmi et al. 2017); band 8 is panchromatic, taking images in the wide visible wavelength range (0,503-0,676 μm) with 15 m spatial resolution. These bands allow obtaining various kinds of information on the characteristics of the land surface, including vegetation cover. Two spectral bands for infrared wavelength are collected by the TIRS instrument. In previous sensors (TM and ETM +), these were covered by a single band: band 10 (TIRS 1, 10.6-11.19 μm) and band 11 (TIRS 2, 11.5-12.51 μm), both with 100 m spatial resolution (Tab. 1) (NASA, 2018). In terms of tracking/analyzing climate and environmental issues, the Landsat database has proven to be quite useful to use (Alavipanah et al. 2010; Adeyeri et al. 2017; Mfondum et al. 2016; Narayan et al. 2016). It should be noted that to formulate surface-atmosphere connections, a key factor is LST (Dickinson, 1983; Adeyeri et al. 2017; Sobrino et al. 2004b; Sobrino et al. 2003; Sobrino et al. 2004a).

Fig. 3 shows the work steps in a general way, while the details for each step taken will be presented in the following sections. As can be seen from Tab. 2, the image used in our study was cloudless. Given that the above image is downloaded for free, it makes it more cost-effective and much more efficient. This data, after downloading, was georeferenced and cut only for our study area (analysis is easier – less load in our software – ArcGIS 10.5) (Berila and Isufi, 2021b).

Tab. 1 Operational Land Imager (OLI) and Thermal Infrared Sensor (TIRS) (Landsat 8) spectral bands

Spectral Band	Wavelength (μm)	Spatial Resolution (m)
Band 1 – Coastal/Aerosol	0.435-0.451	30
Band 2 – Blue	0.452-0.512	30
Band 3 – Green	0.533-0.590	30
Band 4 – Red	0.636-0.673	30
Band 5 – NIR	0.851-0.879	30
Band 6 – SWIR 1	1.566-1.651	30
Band 7 – SWIR 2	2.107-2.294	30
Band 8 – Panchromatic	0.503-0.676	15
Band 9 – Cirrus	1.363-1.384	30
Band 10 – TIRS 1	10.60-11.19	100
Band 11 – TIRS 2	11.50-12.51	100

Source: Compiled by authors

Tab. 2 Characteristics of the satellite image used in this study

Sensor type	Date	Path/ row	Cloud cover	Spatial resolution	Format	Source
Landsat 8 OLI/TIRS	2019/07/02	185/30	0%	30 m	Tiff	https://earthexplorer.usgs.gov/

Source: Compiled by authors

In Landsat 8 sensor satellite images, thermal data is stored in the form of digital numbers (DN). These numbers represent cells (pixels) that have not yet been calibrated into units (Käfer et al. 2020) that make sense (meaningful units). After taking satellite images, the first process or task is to return the digital numbers to radiance. The following equation was used to convert DNs to spectral radiance (USGS, 2019) in the Landsat 8 TIRS sensor (Guha and Govil, 2020; Berila and Isufi, 2021b):

$$L_\lambda = M_L \times Q_{cal} + A_L \qquad (1)$$

where:
L_λ is TOA spectral radiance ($Watss/(m^2 \times srad \times \mu m)$), M_L is Band-specific multiplicative rescaling factor from the metadata, Q_{cal} is Quantized and calibrated standard product pixel values (DN), A_L is Band-specific additive rescaling factor from the metadata (Guha and Govil, 2020; Berila and Isufi, 2021b). The metadata of the satellite image is presented in Tab. 3.

Although from the beginning of its operation TIRS has proven to be stable, still there were some elements (objects) that are hung in the image like errors in cali-

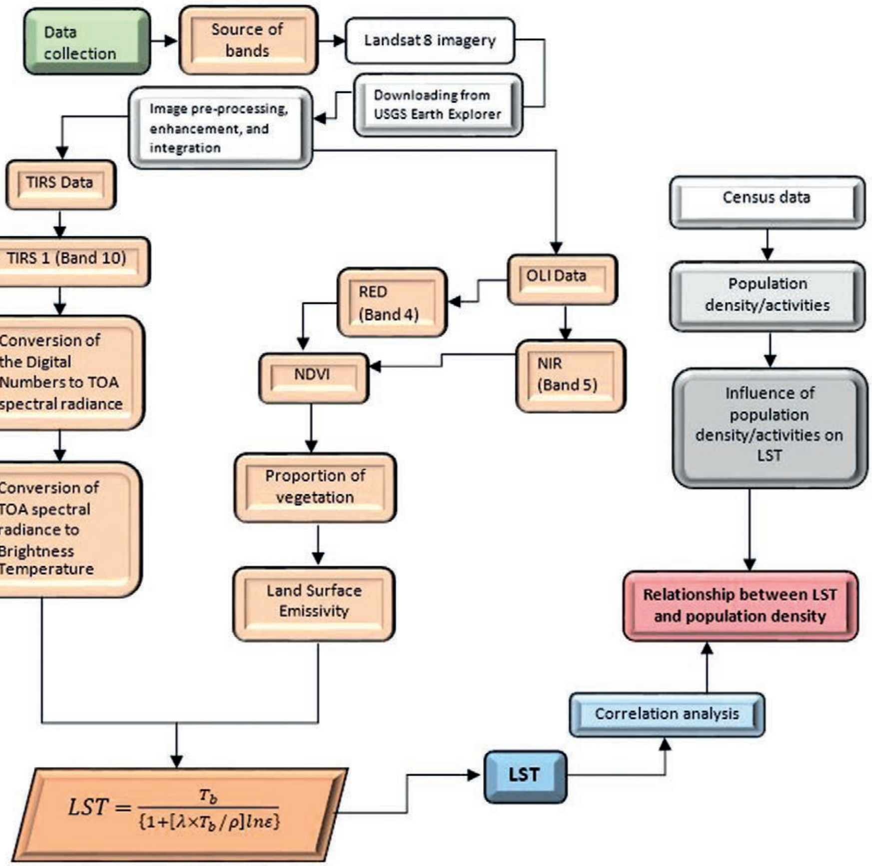

Fig. 3
Flowchart depicting methodology
Source: Compiled by authors

bration and banding (Montanaro et al. 2014). Such a thing is caused by stray light effects. The impacts of these 2 effects are smaller in band 10 compared to band 11. Based on the numerous analyzes and studies that have been done, it has been concluded that band 10 of TIRS data is better and should be used instead of band 11. This, due to the good performance shown by band 10 (Montanaro et al. 2014; Adeyeri et al. 2017). For this study, TIRS band 10 was used.

Calculation of brightness temperature

The next step is to use the constant values given in the metadata in order to convert the spectral radiation to brightness temperature (T_b). In order to convert the radiance to brightness temperature, equation (2) has been used in the study (Isaya Ndossi and Avdan, 2016; USGS, 2019):

$$T_b = \frac{K_2}{\ln\left[\frac{K_1}{L_\lambda}+1\right]} \qquad (2)$$

where:
T_b is the at-sensor brightness temperature [K], L_λ is the spectral radiance of thermal band 10 [$Wm^{-2}sr^{-1}\mu m^{-1}$], K_1 is the band-specific thermal conversion constant from the metadata and K_2 band-specific thermal conversion constant from the metadata. The same equation is used for all sensors. The K_1 and K_2 values may vary depending on the sensor and the wavelengths by which the thermal bands operate (Isaya Ndossi and Avdan, 2016). The values of K_1 and K_2 can be obtained from the metadata file of the scene.

Tab. 3 Metadata of the satellite image

Band	Variable	Description	Value
10		Thermal band	
	K_1	Thermal constant	774.8853
	K_2		1321.0789
	M_L	Band-specific multiplicative rescaling factor	3.3420E-04
	A_L	Band-specific additive rescaling factor	0.10000

Source: Compiled by authors

Estimation of land surface emissivity

To calculate the LST, it is necessary to evaluate the emissivity of the land surface (LSE) through the NDVI method (Jiménez-Muñoz et al. 2006; Valizadeh Kamran et al. 2015). $d\varepsilon$ is the effect of the geometrical distribution of natural surfaces and internal reflections (Sobrino et al. 2004a; Igun and Williams, 2017). To calculate the emissivity we rely on the following equation (Guha and Govil, 2020):

$$d\varepsilon = (1 - \varepsilon_s)(1 - F_v)\, F_{\varepsilon_v} \qquad (3)$$

where ε_v is vegetation emissivity, ε_s is soil emissivity, F_v is fractional vegetation and F is a shape factor whose mean is 0.55 (Igun and Williams, 2017; Sobrino et al. 2004a; Guha and Govil, 2020).

$$\varepsilon = \varepsilon_v \times F_v + \varepsilon_s (1 - F_v) + d\varepsilon \qquad (4)$$

where ε is emissivity. From Equations (3) and (4), ε may be determined by the following equation (Yuvaraj, 2020):

$$\varepsilon = 0.004 \times F_v + 0.989 \qquad (5)$$

The proportion of vegetation (F_v) is calculated based on the following equation (Wang et al. 2015):

$$F_v = \left[\frac{NDVI - NDVI_{min}}{NDVI_{max} - NDVI_{min}}\right]^2 \quad (6)$$

The following equation is used to calculate NDVI with the help of Landsat visible (band 4) and NIR (band 5) images (Yuvaraj, 2020):

$$NDVI = \frac{NIR - R}{NIR + R} = \frac{band\ 5 - band\ 4}{band\ 5 + band\ 4} \quad (7)$$

where NIR and RED are the near-infrared and red band pixel values respectively (Alemu, 2019). The value of NDVI ranges between -1.0 and 1.0 (Alemu, 2019). High NDVI values indicate healthy vegetation while low values indicate less or no vegetation.

Calculation of LST

The final step of estimating the LST is as follows (Weng et al. 2004; Alemu, 2019):

$$LST = \frac{T_b}{\{1 + [\lambda \times T_b / \rho] ln\varepsilon\}} \quad (8)$$

Where:
λ is the wavelength of emitted radiance by Landsat 8 which is 10.8 (given by NASA), ε is the land surface emissivity, and ρ is given by the following equation (Yuvaraj, 2020):

$$\rho = h\frac{c}{\sigma} = 14388\ \mu m\ K \quad (9)$$

where h is Planck's constant (6.626×10^{-34} Js), σ is the Boltzmann constant (1.38×10^{-23} J/K), and c is the velocity of light (2.988×10^{8} m/s) (Alemu, 2019).

RESULTS AND DISCUSSION

In our study area, from the spatial distribution of LST, it was observed that the pixels with high LST values correspond to the areas which have little or no vegetation cover. Such areas are bare surfaces and built-up areas. Whereas, the pixels that recorded the lowest LST values were those that corresponded to the surfaces where the vegetation and water bodies stood out. So, the high values of LST stand out in the areas that do not have vegetation and such a thing is best seen in Figure 4.

Figure 4 shows that LST values range from 296,485 K to 317,848 K. The pixels with the highest LST values lie in the western part of our study area in which the vast majority of built-up areas are located. Also, pixels with high values are clearly seen in the southern part because in this area are found bare surfaces, which are considered as one of the generators of the SUHI phenomenon.

The relationship between LST and population density is very important to understand. The lowest values of LST have dense vegetation as well as water bodies.

While, on the other hand, the highest values of LST have the built areas. Also, it is very important to note that high LST values have bare surfaces. This is because the solar energy that falls on this type of surface is completely absorbed by a thin layer of it. Therefore, if the bare surface is compared to the water body, then the bare surface will heat up much more due to its lower specific heat capacity. Thus, if we make a comparison between natural and artificial surfaces (built-up areas) we will notice that the latter conserve solar energy while natural surfaces maintain low temperatures due to greater reflection of radiation.

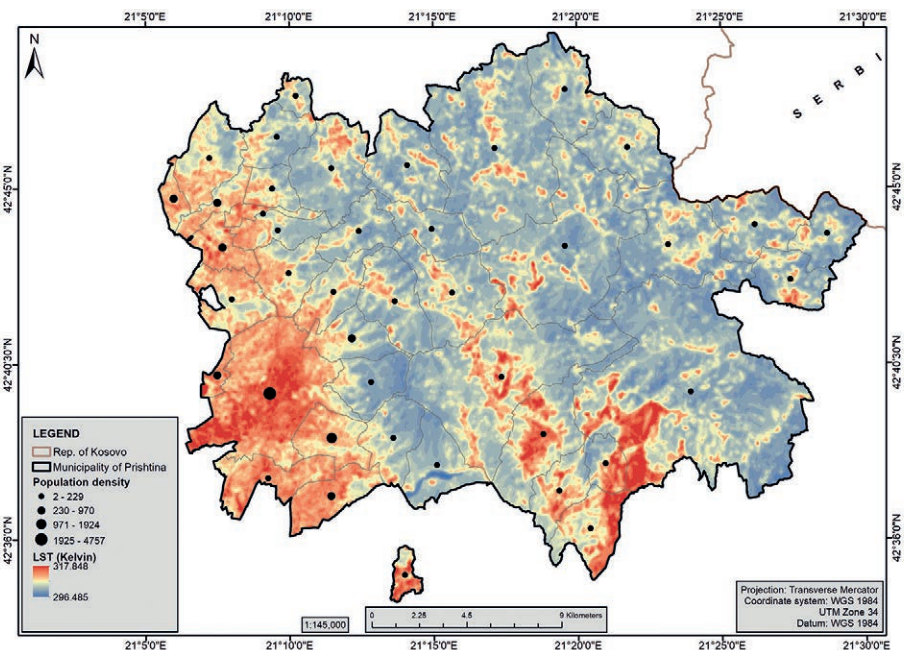

Fig. 4
Spatial distribution of LST and population density of Prishtina
Source: Compiled by authors

The upward trend of LST with increasing population density is shown in Figure 5. The values of the correlation coefficient (r) between LST and population density is 0.768005 showing a strong positive correlation. So, in other words, the areas in which the population density is high, will inevitably cause an increase in LST values due to the activities undertaken. In these areas, the population, as a result of high density, made a number of changes as a result of increasing demand. The most striking changes are the substitution of natural materials with artificial ones and the excessive use of low albedo materials. All these actions are done as a result of an irregularity in the planning of the city. If such a situation continues like this, the values of LST will continue to grow, endangering the health of the population of Prishtina.

Kosovo, like other countries in the region, faces environmental pollution and environmental degradation. This bad condition causes an extremely large amount of greenhouse gases to accumulate. The large number of human activities (commercial, industrial, vehicles, etc.) that take place in Prishtina causes the level of pollution to be high – consequently the level of greenhouse gases increases. This high level of these gases makes the long-wave radiation not be able to leave but stay on the ground causing the LST values to increase.

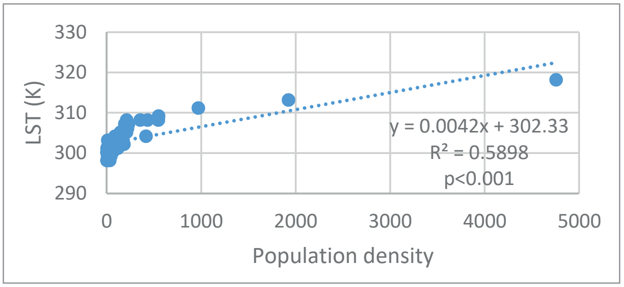

Fig. 5
Scatter plot between LST and population density
Source: Compiled by authors

For the sake of significant political, social, and economic changes during certain periods of time, Prishtina has experienced fluctuations in economic, cultural, and social development. Today Prishtina faces many challenges in managing its territory and resources. In legal terms, the inadequacy of programs addressing planning and environmental issues has led to uncontrolled urban expansion and changes in the physical environment. Developmental challenges in terms of the physical environment are mainly related to the natural environment and environmental degradation such as pollution and degradation of the environment, insufficient and irrational use of natural resources, usurpation of agricultural land for construction purposes, agricultural land loss, urban flood and uncontrolled and unplanned urban expansion. The biggest environmental challenge of the Municipality of Prishtina is the irrational use of natural resources, which results in pollution and degradation of the environment, which is affecting the further strengthening of the SUHI phenomenon. The unplanned development of agricultural land resulting from the use of it for construction with impervious materials has resulted in a major loss – it should be borne in mind that any change and replacement of natural to artificial areas only contributes to the deterioration of the situation with SUHI.

The impact and importance of vegetation on the earth's surface is extraordinary and can never be minimized. First, it affects the albedo of the earth, and, secondly it affects the LST. Vegetation, in the area where it appears, affects the freshness of the environment or, more precisely, cools the environment and reduces the concentration of CO_2 in the atmosphere, thus reducing the SUHI effect (Ebenezer et al. 2016). Therefore, the greater use of green areas will help in countering the SUHI phenomenon. Illegal construction in urban and rural areas results in uncontrolled urban expansion that must be prevented in order to achieve better development. If the uncontrolled urban expansion in Prishtina continues, the generations to come will have even more serious problems with the SUHI phenomenon.

CONCLUSIONS

This study of ours shows very clearly the spatial distribution of LST and its difference throughout Prishtina. Making the overlap in the LST map of population density, it is clear that the latter has an extraordinary role (main role) in increasing the surface temperature of the earth, strengthening the intensity of the UHI phenomenon, and, thus, creating the microclimate of Prishtina.

The data of Landsat 8 OLI and TIRS, dated 2 July 2019 were used to evaluate the SUHI effect through the spatial model of LST and its relation with population density. For the whole territory of Prishtina, LST showed a strong relationship with vegetation, highlighting the great role that vegetation has in reducing the SUHI effect. High positive correlation values were shown by the analysis of the correlation between LST and population density. Thus, once again, the strong role that the population has with its activities in further strengthening the SUHI effect is emphasized. SUHI areas were identified through the determination of LST. These areas spread mainly along the western part due to the built-up areas and in the bare surfaces in the southern part. Based on the results of the study, we conclude that responsible for generating the SUHI effect in Prishtina are the high population density and bare surfaces.

For many scientists around the world, but also for many environmental planners, assessing the SUHI effect is now the main concern given the growing trends of urbanization and urban temperature as well as the adverse effects they cause on the population globally. The importance of environmental greenery in urban planning should always be emphasized because vegetation has the ability to reduce the SUHI effect. For many cities around the world, the problem with the SUHI effect is a very sensitive issue because these cities have been facing it for a long time. In each city, administrators must take a series of steps regarding land planning and use, creating cool areas within the city with the sole purpose of promoting sustainable development and improving the lives of citizens.

This study shows how SUHI maps can provide an extraordinary tool to identify areas in which the SUHI effect is very high and causes concern to the people living there. Furthermore, municipal administrators can take a series of mitigation measures against the SUHI effect, such as materials with a high albedo, creation of green and cool areas, application of green roofs, and a series of other actions which will lead to a better life.

In order to make the right/correct addresses and assess the issue of microclimate, and also to maximize the impact that the UHI effect has on the city and its inhabitants, the results of such types of studies should be taken very seriously because can be quite helpful in minimizing such negative effects.

REFERENCES

ADEYERI, O.E., AKINSANOLA, A.A., & ISHOLA, K.A. (2017). Investigating surface urban heat island characteristics over Abuja, Nigeria: Relationship between land surface temperature and multiple vegetation indices. *Remote Sensing Applications: Society and Environment*, 7, 57-68. https://doi.org/10.1016/j.rsase.2017.06.005.

ALAVIPANAH, S.K., SARADJIAN, M., SAVAGHEBI, G.R., KOMAKI, C.B., MOGHIMI, E., KARIMPURREYHAN, M. (2010). Land surface temperature in the yardang region of Lut desert (Iran) based on field measurements and landsat thermal data. *Journal of Agricultural Science and Technology*, 9, 287-303.

ALEMU, M.M. (2019). Analysis of Spatio-Temporal Land Surface Temperature and Normalized Difference Vegetation Index Changes in the Andassa Watershed, Blue Nile Basin, Ethiopia. *Journal of Resources and Ecology*, 10(1), 77. https://doi.org/10.5814/j.issn.1674-764x.2019.01.010.

BERILA, A., & ISUFI, F. (2021a). Determination of dissection index (di) using GIS & RS techniques: a case study on Drenica river basin. *Folia Geographica*, 63(1), 5-18.

BERILA, A., & ISUFI, F. (2021b). Two Decades (2000–2020) Measuring Urban Sprawl Using GIS, RS and Landscape Metrics: a Case Study of Municipality of Prishtina (Kosovo). *Journal of Ecological Engineering*, 22(6), 114-125. https://doi.org/10.12911/22998993/137078.

BUYANTUYEV, A., & WU, J. (2009). Urban heat islands and landscape heterogeneity: linking spatiotemporal variations in surface temperatures to land-cover and socioeconomic patterns. *Landscape Ecology*, 25(1), 17-33. http://dx.doi.org/10.1007/s10980-009-9402-4.

CLAY, R., GUAN, H., WILD, N., BENNETT, J., VINODKUMAR, & EWENZ, C. (2016). Urban Heat Island traverses in the City of Adelaide, South Australia. *Urban Climate*, 17, 89-101. http://dx.doi.org/10.1016/j.uclim.2016.06.001.

DESPINI, F., FERRARI, C., BIGI, A., LIBBRA, A., TEGGI, S., MUSCIO, A., & GHERMANDI, G. (2016). Correlation between remote sensing data and ground based measurements for solar reflectance retrieving. *Energy and Buildings*, 114, 227-233. http://dx.doi.org/10.1016/j.enbuild.2015.06.018.

DICKINSON, R.E. (1983). Land Surface Processes and Climate – Surface Albedos and Energy Balance. *Theory of Climate, Proceedings of a Symposium Commemorating the Two-Hundredth Anniversary of the Academy of Sciences of Lisbon*, 305-353. http://dx.doi.org/10.1016/s0065-2687(08)60176-4.

EBENEZER, A.O., EMMANUEL, C.O., & FRANK, O.A. (2016). Mapping Evapotranspiration for different Landcover in the Lake Chad Region of Nigeria using Landsat Datasets. *Journal of Remote Sensing Technology*, 4(1), 58-69. https://doi.org/10.18005/jrst0401005.

ENVIRONMENTAL PROTECTION AGENCY (EPA). (2017). Reducing Urban Heat Islands: Compendium of Strategies; US Environmental Protection Agency: Washington, DC, USA [accessed on 18 March 2021]. Retrieved from: https://www.epa.gov/sites/production/files/2014-06/documents/basicscompendium.pdf.

FABRIZI, R., BONAFONI, S., & BIONDI, R. (2010). Satellite and Ground-Based Sensors for the Urban Heat Island Analysis in the City of Rome. *Remote Sensing*, 2(5), 1400-1415. http://dx.doi.org/10.3390/rs20514.

GUHA, S., & GOVIL, H. (2020). Land surface temperature and normalized difference vegetation index relationship: a seasonal study on a tropical city. *SN Applied Sciences*, 2(10). https://doi.org/10.1007/s42452-020-03458-8.

HARLAN, S.L., & RUDDELL, D.M. (2011). Climate change and health in cities: impacts of heat and air pollution and potential co-benefits from mitigation and adaptation. *Current Opinion in Environmental Sustainability*, 3(3), 126-134. http://dx.doi.org/10.1016/j.cosust.2011.01.001.

IGUN, E., & WILLIAMS, M. (2018). Impact of urban land cover change on land surface temperature. *Global Journal of Environmental Science and Management*, 4, 47-58. https://doi.org/10.22034/gjesm.2018.04.01.005.

ISAYA NDOSSI, M., & AVDAN, U. (2016). Application of Open Source Coding Technologies in the Production of Land Surface Temperature (LST) Maps from Landsat: A PyQGIS Plugin. *Remote Sensing*, 8(5), 413. https://doi.org/10.3390/rs8050413.

ISUFI, F., BERILA, A. (2021). Using geospatial technology to analyse land use/cover changes in Prishtina, Kosovo (2000–2020). *GeoJournal*. https://doi.org/10.1007/s10708-021-10452-z.

JEEVALAKSHMI, D., NARAYANA REDDY, S., & MANIKIAM, B. (2017). Land Surface Temperature Retrieval from LANDSAT data using Emissivity Estimation. *International Journal of Applied Engineering Research*, 12(20), 9679-9687.

JIMÉNEZ-MUÑOZ, J.C., SOBRINO, J.A., GILLESPIE, A., SABOL, D., & GUSTAFSON, W. T. (2006). Improved land surface emissivities over agricultural areas using ASTER NDVI. *Remote Sensing of Environment*, 103(4), 474-487. http://dx.doi.org/10.1016/j.rse.2006.04.012.

KAMUSOKO, C., & ANIYA, M. (2007). Land use/cover change and landscape fragmentation analysis in the Bindura District, Zimbabwe. *Land Degradation & Development*, 18(2), 221-233. https://doi.org/10.1002/ldr.761.

KAMUSOKO, C., ANIYA, M. (2009). Hybrid classification of Landsat data and GIS for land use/cover change analysis of the Bindura district, Zimbabwe. *International Journal of Remote Sensing*, 30(1), 97-115. https://doi.org/10.1080/01431160802244268.

KAS (KOSOVO AGENCY OF STATISTICS). (2012). People on the move: an analysis of international, national and local mobility of Kosovo people [accessed on 10 March 2021]. Retrieved from: https://ask.rks-gov.net/media/1285/people-on-the-move-eng.pdf.

KAS (KOSOVO AGENCY OF STATISTICS). (2014). Kosovan Migration, Prishtina [accessed on 1 March 2021]. Retrieved from: https://ask.rks-gov.net/media/1380/kosovan-migration-2014.pdf.

KAS (KOSOVO AGENCY OF STATISTICS). (2020). Statistical yearbook of the Republic of Kosovo, Prishtina [accessed on 10 February 2021]. Retrieved from: https://ask.rks-gov.net/media/5629/vjetari-final-2020-per-web.pdf.

KÄFER, P.S., ROLIM, S.B.A., DIAZ, L.R., ROCHA, N.S. DA, IGLESIAS, M.L., & REX, F.E. (2020). Comparative analysis of split-window and single-channel algorithms for land surface temperature retrieval of a pseudo-invariant target. *Boletim de Ciências Geodésicas*, 26(2). https://doi.org/10.1590/s1982-21702020000200008.

KITYUTTACHAI, K., TRIPATHI, N.K., TIPDECHO, T., & SHRESTHA, R. (2013). CA-Markov analysis of constrained coastal urban growth modeling: Hua Hin seaside city, Thailand. *Sustainability*, 5(4), 1480-1500. https://doi.org/10.3390/su5041480.

LEE, Y., & CHANG, H. (2011). The simulation of land use change by using CA-Markov model: a case study of Tainan City, Taiwan. *19th International Conference on Geoinformatics*, 24-26 June, 1-4. https://doi.org/10.1109/geoinformatics.2011.5980819.

LIU, Y., HOU, S., KONG, X. & XU, Y. (2011). The analysis on land use change in urban fringe area based on the GIS technology. *International Conference on Remote Sensing, Environment and Transportation Engineering*, 6444-6447. https://doi.org/10.1109/rsete.2011.5965832.

MAVROGIANNI, A., DAVIES, M., BATTY, M., BELCHER, S., BOHNENSTENGEL, S., CARRUTHERS, D., CHALABI, Z., CROXFORD, B., DEMANUELE, C., EVANS, S., GIRLDHARAN, R., HACKER, J., HAMILTON, I., HOGG, C., HUNT, J., KOLOKOTRONI, M., MARTIN, C., MILNER, J., RAJAPAKSHA, I., … YE, Z. (2011). The comfort, energy and health implications of London's urban heat island. *Building Services Engineering Research and Technology*, 32(1), 35-52. http://dx.doi.org/10.1177/0143624410394530.

MOGHADAM, H.H., & HELBICH, M. (2013). Spatiotemporal urbanization processes in the megacity of Mumbai, India: a Markov chains-cellular automata urban growth model. *Applied Geography*, 40, 140-149. https://doi.org/10.1016/j.apgeog.2013.01.009.

MOHAJERANI, A., BAKARIC, J., & JEFFREY-BAILEY, T. (2017). The urban heat island effect, its causes, and mitigation, with reference to the thermal properties of asphalt concrete. *Journal of Environmental Management*, 197, 522-538. http://dx.doi.org/10.1016/j.jenvman.2017.03.095.

MONTANARO, M., GERACE, A., LUNSFORD, A., & REUTER, D. (2014). Stray Light Artifacts in Imagery from the Landsat 8 Thermal Infrared Sensor. *Remote Sensing*, 6(11), 10435-10456. http://dx.doi.org/10.3390/rs61110435.

MOREFIELD, P., FANN, N., GRAMBSCH, A., RAICH, W., & WEAVER, C. (2018). Heat-Related Health Impacts under Scenarios of Climate and Population Change. *International Journal of Environmental Research and Public Health*, 15(11), 2438. http://dx.doi.org/10.3390/ijerph15112438.

MUBEA, K., NGIGI, T., & MUNDIA, C. (2011). Assessing Application of Markov Chain Analysis in Nakuru. *Applied Geoinformatics for Society and Environment*, 182-188.

MUNICIPALITY OF PRISHTINA. (2013). Municipal Development Plan of Prishtina 2012–2022 [accessed on 21 January 2021]. Retrieved from: https://prishtinaonline.com/uploads/prishtina_pzhk_2012-2022_shqip%20(1).pdf.

NARAYAN, K., KHANINDRA, P., ABHISEK, C., & SAHOO, S. (2016). Urban heat island explored by corelationship between land surface temperature vs multiple-vegetation indices. *Spatial Information Research*, 24, 515-529. http://dx.doi.org/10.1007/s41324-016-0049-3.

NASA. (2018). Landsat Science: Landsat 8 Overview [accessed on 28 January 2021]. Retrieved from: https://landsat.gsfc.nasa.gov/landsat-8/landsat-8-overview/.

NGANDAM MFONDOUM, A.H., ETOUNA, J., NONGSI, B.K., MVOGO MOTO, F.A., … NOULAQUAPE DEUSSIEU, F.G. (2016). Assessment of Land Degradation Status and Its Impact in Arid and Semi-Arid Areas by Correlating Spectral and Principal Component Analysis Neo-Bands. *International Journal of Advanced Remote Sensing and GIS*, 5(1), 1539-1560. https://doi.org/10.23953/cloud.ijarsg.77.

NICHOL, J.E., FUNG, W.Y., LAM, K., & WONG, M.S. (2009). Urban heat island diagnosis using ASTER satellite images and "in situ" air temperature. *Atmospheric Research*, 94(2), 276-284. http://dx.doi.org/10.1016/j.atmosres.2009.06.011.

NURUZZAMAN, M. (2015). Urban Heat Island: Causes, Effects and Mitigation Measures - A Review. *International Journal of Environmental Monitoring and Analysis*, 3(2), 67. https://doi.org/10.11648/j.ijema.20150302.15.

O'MALLEY, C., PIROOZFARB, P.A.E., FARR, E.R.P., & GATES, J. (2014). An Investigation into Minimizing Urban Heat Island (UHI) Effects: A UK Perspective. *Energy Procedia*, 62, 72-80. https://doi.org/10.1016/j.egypro.2014.12.368.

OKE, T.R. (1987). *Boundary layer climates*. London: Routledge.

PERES, L.F., LUCENA, A.J., ROTUNNO FILHO, O.C., & FRANÇA, J.R. (2018). The urban heat island in Rio de Janeiro, Brazil, in the last 30 years using remote sensing data. *International Journal of Applied Earth Observation and Geoinformation*, 64, 104-116. http://dx.doi.org/10.1016/j.jag.2017.08.012.

PLLANA, R. (2015). *Kosovo climate*. Prishtina: KASA. (In Albanian).

POUR, T. & VOŽENÍLEK, V. (2020). Thermal data analysis for urban climate research: A case study of Olomouc, Czechia. *Geographia Cassoviensis*, 14(1), 77-91. http://dx.doi.org/10.33542/gc2020-1-05.

ROTH, M., OKE, T.R., & EMERY, W.J. (1989). Satellite-derived urban heat islands from three coastal cities and the utilization of such data in urban climatology. *International Journal of Remote Sensing*, 10(11), 1699-1720. http://dx.doi.org/10.1080/01431168908904002.

SANTAMOURIS, M., SYNNEFA, A., & KARLESSI, T. (2011). Using advanced cool materials in the urban built environment to mitigate heat islands and improve thermal comfort conditions. *Solar Energy*, 85(12), 3085-3102. http://dx.doi.org/10.1016/j.solener.2010.12.023.

SHERAFATI, S., SARADJIAN, M.R. & RABBANI, A. (2018). Assessment of Surface Urban Heat Island in Three Cities Surrounded by Different Types of Land-Cover Using Satellite Images. *Journal of the Indian Society of Remote Sensing*, 46, 1013-1022. https://doi.org/10.1007/s12524-017-0725-3.

SCHWARZ, N., SCHLINK, U., FRANCK, U., & GROßMANN, K. (2012). Relationship of land surface and air temperatures and its implications for quantifying urban heat island indi-cators – An application for the city of Leipzig (Germany). *Ecological Indicators*, 18, 693-704. http://dx.doi.org/10.1016/j.ecolind.2012.01.001.

SMOLIAK, B.V., SNYDER, P.K., TWINE, T.E., MYKLEBY, P.M., & HERTEL, W.F. (2015). Dense Network Observations of the Twin Cities Canopy-Layer Urban Heat Island. *Journal of Applied Meteorology and Climatology*, 54(9), 899-1917. http://dx.doi.org/10.1175/jamc-d-14-0239.1.

SOBRINO, J.A., CORRESPOND, JIMÉNEZ-MUÑOZ, J.C., EL-KHARRAZ, J., GÓMEZ, M., ROMAGUERA, M., & SÓRIA, G. (2004b). Single-channel and two-channel methods for land surface temperature retrieval from DAIS data and its application to the Barrax site. *International Journal of Remote Sensing*, 25(1), 215-230. http://dx.doi.org/10.1080/0143116031000115210.

SOBRINO, J.A., EL-KHARRAZ, J., & LI, Z.-L. (2003). Surface temperature and water vapour retrieval from MODIS data. *International Journal of Remote Sensing*, 24(24), 5161-5182. http://dx.doi.org/10.1080/0143116031000102502.

SOBRINO, J.A., JIMÉNEZ-MUÑOZ, J.C., & PAOLINI, L. (2004a). Land surface temperature retrieval from LANDSAT TM 5. *Remote Sensing of Environment*, 90(4), 434-440. http://dx.doi.org/10.1016/j.rse.2004.02.003.

SUDHIRA, H.S., RAMACHANDRA, T. & JAGADISH, K. (2003). Urban sprawl pattern recognition and modeling using GIS. *Map India Conference*, 28-31.

TAHA, H. (1997). Urban climates and heat islands: albedo, evapotranspiration, and anthropogenic heat. *Energy and Buildings*, 25(2), 99-103. https://doi.org/10.1016/s0378-7788(96)00999-1.

TALOOR, A.K., DRINDER SINGH MANHAS, & CHANDRA KOTHYARI, G. (2021). Retrieval of land surface temperature, normalized difference moisture index, norma-

lized difference water index of the Ravi basin using Landsat data. *Applied Computing and Geosciences*, 9, 100051. https://doi.org/10.1016/j.acags.2020.100051.
UNHABITAT. (2016). Urbanisation and Development: Emerging Futures. World Cities Report 2016: United Nations Human Settlements Programme [accessed on 25 January 2021]. Retrieved from: https://unhabitat.org/sites/default/files/download-manager-files/WCR-2016-WEB.pdf.
UNITED NATIONS (UN). (2016). The world cities in 2016 [accessed on 29 January 2021]. Retrieved from: https://www.un.org/en/development/desa/population/publications/pdf/urbanization/the_worlds_cities_in_2016_data_booklet.pdf.
USGS. (2019). Using the USGS Landsat 8 Product [accessed on 5 March 2021]. Retrieved from: https://prd-wret.s3.us-west-2.amazonaws.com/assets/palladium/production/atoms/files/LSDS-1574_L8_Data_Users_Handbook-v5.0.pdf.
VALIZADEH KAMRAN, K., PIRNAZAR, M., & FARHADI BANSOULEH, V. (2015). Land surface temperature retrieval from Landsat 8 TIRS: comparison between split window algorithm and SEBAL method. *Third International Conference on Remote Sensing and Geoinformation of the Environment* (RSCy2015). https://doi.org/10.1117/12.2192491.
VOOGT, J. (2008). How Researchers Measure Urban Heat Islands [accessed on 11 March 2021]. Retrieved from: https://19january2017snapshot.epa.gov/sites/production/files/2014-07/documents/epa_how_to_measure_a_uhi.pdf.
VOOGT, J.A., & OKE, T. R. (2003). Thermal remote sensing of urban climates. *Remote Sensing of Environment*, 86(3), 370-384. http://dx.doi.org/10.1016/s0034-4257(03)00079-8.
WANG, F., QIN, Z., SONG, C., TU, L., KARNIELI, A., & ZHAO, S. (2015). An Improved Mono-Window Algorithm for Land Surface Temperature Retrieval from Landsat 8 Thermal Infrared Sensor Data. *Remote Sensing*, 7(4), 4268-4289. http://dx.doi.org/10.3390/rs7.
WANG, H., ZHANG, Y., TSOU, J., & LI, Y. (2017). Surface Urban Heat Island Analysis of Shanghai (China) Based on the Change of Land Use and Land Cover. *Sustainability*, 9(9), 1538. http://dx.doi.org/10.3390/su9091538.
WENG, Q., LU, D., & SCHUBRING, J. (2004). Estimation of land surface temperature–vegetation abundance relationship for urban heat island studies. *Remote Sensing of Environment*, 89(4), 467-483. http://dx.doi.org/10.1016/j.rse.2003.11.005.
YUAN, F., & BAUER, M.E. (2007). Comparison of impervious surface area and normalized difference vegetation index as indicators of surface urban heat island effects in Landsat imagery. *Remote Sensing of Environment*, 106(3), 375-386. https://doi.org/10.1016/j.rse.2006.09.003.
YUVARAJ, R.M. (2020). Extents of Predictors for Land Surface Temperature Using Multiple Regression Model. *The Scientific World Journal*, 2020, 1-10. https://doi.org/10.1155/2020/3958589.